ELSEVIER

Computational and Theoretical Polymer Science 9 (1999) 197–202

Computational and Theoretical Polymer Science

Elasticity of polydiene networks in tension and compression

C.M. Roland[a,*], P.H. Mott[b], G. Heinrich[c]

[a]Chemistry Division, Code 6120, Naval Research Laboratory, Washington, DC 20375-5342, USA
[b]Geo-Centers, Inc., Ft. Washington, MD, USA
[c]Continental AG Strategic Tire Technology Materials Research, Postfach 169 D, 30001 Hanover, Germany

Received 16 November 1998; received in revised form 4 January 1999; accepted 4 January 1999

Abstract

Previously we reported experimental data, on natural rubber networks in tension and compression, which deviated from the constraint models of rubber elasticity. Equivalent experiments were carried out on crosslinked polybutadiene, and similar discrepancies with theory observed. An alternative approach, based on the tube model of chain entanglements, was found to provide a more accurate description of the experimental data. However, physical interpretation of the values for the model's parameters is problematic. Published by Elsevier Science Ltd.

Keywords: Polydiene networks; Elasticity; Tension and compression

1. Introduction

Developing constitutive equations which accurately describe the elastic response of elastomers is an essential part of understanding the behavior of this important class of materials. Constitutive equations also have also practical value, for example in the finite-element modeling of rubber. Although phenomenological expressions may serve the latter purpose well, they cannot offer insights into the origin of rubber elasticity. This requires molecular-based theories.

We have recently carried out experiments in which both extension and compression data were obtained on the same sample test pieces [1]. Results for natural rubber networks [2,3] revealed that, while molecular theories of rubber elasticity fit the data well for a single mode of deformation, discrepancies arise when compression and tension results are analyzed together. In this paper we report results for crosslinked polybutadiene, and extend our comparison to a tube-model of elasticity.

2. Background

The value of finding constitutive equations that provide insights into molecular behavior, while also accurately describing experimental results, has long been appreciated [4–7]. The Mooney-Rivlin equation is commonly used to describe results for rubber in tension, although it is not a valid constitutive relation, since its accuracy does not extend to all modes of deformation [6–8]. The popularity of the Mooney-Rivlin equation is due, at least in part, to its simplicity; for the engineering stress,

$$\sigma_{MR} = (2C_1 + 2C_2/\lambda) \times f(\lambda) \quad (1)$$

where λ is the stretch ratio and $f(\lambda) = \lambda - \lambda^{-2}$. When elastomers are subjected to both tension and compression, it is well known that data deviate from Eq. 1 [9,10]. Notwithstanding this failing, as well as the phenomenological basis of the equation, some interpretation of the Mooney-Rivlin parameters in terms of molecular quantities can be made [6,7,11–14]. C_1 is assumed to be proportional to the chemical crosslink density, and C_2 is taken as a measure of entanglement constraints.

If such an interpretation is correct, Eq. 1 shows that the effect entanglements have on stress is alleviated by strain. This idea leads to a general expression having the form

$$\sigma = G_c(1 + h(\lambda)) \times f(\lambda) \quad (2)$$

where the "damping function" $h(\lambda)$ is a decreasing function of strain ($\propto \lambda^{-1}$ for the Mooney-Rivlin equation) [13,15,16]. G_c is the modulus of a phantom network [17,18]

$$G_c = (\nu - \mu)RT \quad (3)$$

having μ junctions and ν elastically active chains per unit

* Corresponding author. Tel.: + 1-202-7671719; fax: + 1-202-7670594.
E-mail address: roland@nrl.navy.mil (C.M. Roland)

1089-3156/99/$ - see front matter. Published by Elsevier Science Ltd.
PII: S1089-3156(99)00005-7

volume. These quantities are related by

$$\nu = \frac{\mu\varphi}{2} \tag{4}$$

where φ is the junction functionality. Eq. 3 represents an extreme of "ideal" behavior, the other being affine deformation, for which $G_c = \nu RT$ [6–8]. These expressions all assume that the primary molecular weight of the network is very large (i.e., chain ends are negligible); otherwise the cycle rank of the network replaces the quantity ν-μ [19].

The concepts underlying Eq. 2 are given a molecular basis in Flory's constrained junction model of rubber elasticity [20,21]. This treatment considers the manner in which neighboring segments sterically hinder the Brownian motion of network junctions. The entanglement contribution to the stress decreases with strain according to

$$h_{cj}(\lambda) = \frac{2}{\varphi - 2}\frac{\lambda K(\lambda_\parallel^2) - \lambda^{-2}K(\lambda_\perp^2)}{f(\lambda)} \tag{5}$$

where the function $K(\lambda^2)$ is defined as

$$K(\lambda^2) = \frac{B\dot{B}}{B+1} + \frac{D\dot{D}}{D+1} \tag{6}$$

with

$$B(\lambda^2) = \frac{\kappa^2(\lambda^2 - 1)}{(\lambda^2 + \kappa)^2} \tag{7}$$

$$\dot{B}(\lambda^2) \equiv \frac{\partial B(\lambda^2)}{\partial(\lambda^2)} = B(\lambda^2)\left[\frac{1}{\lambda^2 - 1} - \frac{2}{\lambda^2 + \kappa}\right] \tag{8}$$

$$D(\lambda^2) = \frac{\lambda^2}{\kappa}B(\lambda^2) \tag{9}$$

and

$$\dot{D}(\lambda^2) \equiv \frac{\partial D(\lambda^2)}{\partial(\lambda^2)} = \frac{1}{\kappa}\left[\lambda^2\dot{B}(\lambda^2) + B(\lambda^2)\right] \tag{10}$$

The parameter κ, assumed to be a constant, quantifies the severity of the constraints on the junction fluctuations.

The constrained junction model was subsequently modified so that the constraints suppressed fluctuations of the chains' mass centers, rather than their junctions [22]. This advancement was generalized in the continuously-constrained chain (CC) model [23,24], which employs the more realistic notion that constraints act all along the chain. The CC model gives

$$h_{cc}(\lambda) = \frac{\varphi}{\varphi - 2}\int_0^1 W(\Theta)\frac{\alpha K(\lambda_\parallel^2) - \alpha^{-2}K(\lambda_\perp^2)}{\alpha - \alpha^{-2}}d\Theta \tag{11}$$

where Θ, which may vary from 0 to 1, is the relative distance from the junction sites (i.e., the distance expressed as a fraction of the strand length), and $W(\Theta)$ is a distribution function describing the distance-dependence of the constraints. If the constraints act uniformly along the chain, $W(\Theta)$ is unity [23]. For the CC model, the constraint parameter $\kappa(\Theta)$ is a function of position

$$\kappa(\Theta) = \kappa\left[1 + \frac{(\varphi - 2)^2\Theta(1 - \Theta)}{\varphi - 1}\right] \tag{12}$$

The topological constraints of the foregoing models are identical to the entanglement constraints governing the low frequency dynamics of polymer melts. The latter are often modeled as a confining tube surrounding the chain [25]. This leads to the idea that the equilibrium modulus of crosslinked rubber includes a contribution from the same interactions that give rise to the plateau modulus, G_N, of the corresponding melt. Thus, Graessley obtained [26]

$$\sigma = (G_c + G_N \times T_e) \times f(\lambda) \tag{13}$$

where T_e is the Langley "trapping factor", equal to the fraction of entanglements whose paths all attach to the network [27,28]. Note that although this expression offers a prediction for the crosslink density, it does not account for the nonlinear elasticity of real networks.

Rubinstein and Panyukov (R-P) [29] expanded on Graessley's approach, by assuming non-affine deformation of the network, whose chains fluctuate within a tube of entanglements. The constitutive result for their model is

$$h_{R-P} = \frac{G_N}{G_c}(\lambda - \lambda^{1/2} + 1)^{-1} \tag{14}$$

whereby all entanglements contribute to the stress (i.e., $T_e = 1$).

An alternative tube model has been proposed Heinrich and coworkers [30–32]. Its principle departure from the approach of Rubinstein and Panyukov is to allow for constraint release. Constraint release is the mitigation of lateral constraints on a chain by Brownian motion of the tube. This effect is believed to be important in the rheology of melts, although the detailed nature of the process is in dispute [25,33–35]. In the conventional use of the term, constraint release is applicable only to melts. In networks, it refers to tube relaxation processes arising from network defects, such as dangling chain ends or an inhomogeneous distribution of junctions.

The constraint release model (CR) yields [30–32]

$$h_{CR} = \frac{G_e}{G_c}\frac{2(\lambda^{\beta/2} - \lambda^{-\beta})}{\beta(\lambda^2 - \lambda^{-1})} \tag{15}$$

where G_e is less than or equal to G_N (i.e., $T_e \leq 1$). The parameter β $(0 \leq \beta \leq 1)$ is a measure of the effect constraint release has on the local deformation. For affine deformation β equals unity, which corresponds to no constraint release.

3. Experimental

Polybutadiene (Budene 1209 from the Goodyear Tire & Rubber Co.) containing 0.44 phr dicumyl peroxide, with 1.0 phr 1,2-dihydro-2,2,4-trimethylquinoline added as an

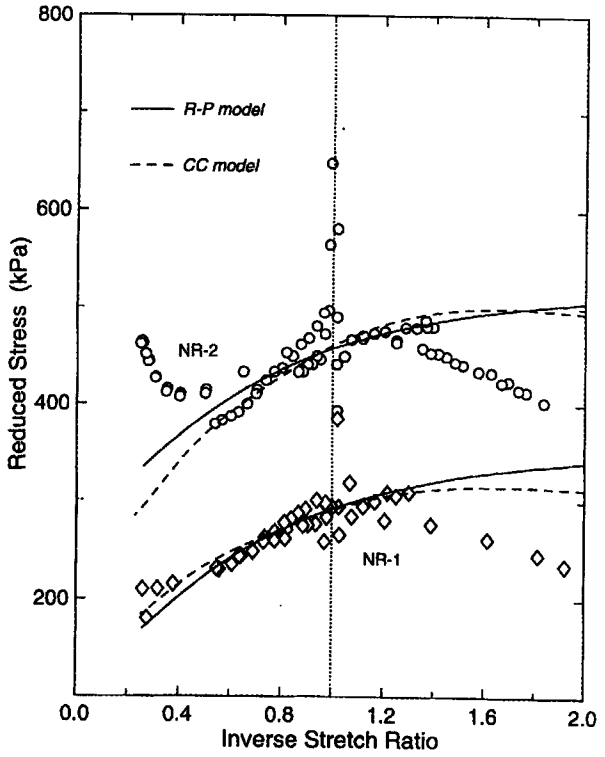

Fig. 1. The stress divided by the strain function f(λ) versus the reciprocal of the stretch ratio for two natural rubber networks crosslinked with 1 (◇◇◇) and 2 (O O O) phr dicumyl peroxide respectively [2,3], along with the respective least-square-fits of the CC model, Eq. 11, (– – –) and the R-P model, Eq. 14 (—) to the extension data. The upturn at high extension for the more cross-linked NR-1, reflecting strain-induced crystallization, is ignored. Neither expression can accurately describe simultaneously both tension and compression results.

antioxidant, was compression molded at 150°C for 120 minutes. Both films (65 × 13 × 1.6 mm) and cylindrical samples (12.2 mm diameter × 17.8 mm high) were prepared. All measurements were carried out at room temperature on neat, unswollen networks.

The apparatus used to obtain compression data on the rubber cylinders is described in detail elsewhere [1]. Bonded cylinders (cyanoacrylate adhesive) were dead-weighted and the consequent change in sample length measured using a linear voltage differential transducer. The correction to the stress due to shear forces at the cylinder ends is given by [36]

$$\sigma = \frac{\sigma_{app}}{\left(\frac{1 + R_0^2}{2H_0^2}\right)} \tag{16}$$

where σ_{app} is the ratio of the applied force to the initial cross-sectional area of the cylinder, σ is the engineering stress corresponding to homogeneous deformation, and R_0 and H_0 are the initial sample radius and height, respectively. A comprehensive assessment demonstrated that Eq. 16 corrects experimental data to an accuracy of better than 5% over substantial ranges of strain [1].

Extension measurements were carried out at small strains ($\lambda \leq 1.8$) by extending cylindrical samples through the use of a screw-driven stage on the sample apparatus used for compression tests. For higher extension, data was obtained on films with attached weights, the resulting strain measured with a cathetometer. Two points were obtained per day, allowing a minimum of 8 hours for the rubber to attain mechanical equilibrium.

We also show herein elastic data for natural rubber networks. Details of these samples and their measurements have been reported [2].

4. Results

4.1. Natural rubber networks

Recently equilibrium mechanical measurements were obtained on natural rubber (NR) networks [2,3], using the experimental technique described above. A comparison of these results to the CC (Eq. 11) and R&P (Eq. 14) models are shown in Fig. 1. The fitted curves conform well to the stress/strain data over a single mode of deformation (e.g., tension); however, the agreement is unsatisfactory when both compression and tension data are considered together.

Although no values for the fitting parameters of these models could improve the agreement with the data, comparisons like those in Fig. 1 are limited by the large scatter in the experimental results. This is primarily due to the ordinate variable, $\sigma/f(\lambda)$, which becomes unstable as λ approaches unity. Interestingly, however, experiments carried out at vanishingly small strains suggested there is a discontinuity near $\lambda = 1$ [37], which would also contribute to the scatter. The noise in the data is absent when the results are plotted simply as the engineering stress versus the strain (Fig. 2).

The data in Fig. 2 has been truncated to $\lambda \leq 2$ to avoid complications from strain-induced crystallization. Also shown are the least-squares fit of the CR model, with the parameters obtained for Eq. 15 listed in Table 1. Since this model includes a third adjustable parameter, some improved agreement with experiment is expected. Nevertheless, systematic deviation from experiment remains.

The natural rubber networks in Figs. 1 and 2 were formed using dicumyl peroxide; therefore, the number of network chains per unit volume can be calculated from the equation of Wood [38]

$$\nu = 7.40 \times 10^{-5} \rho (c - 0.31) \tag{17}$$

where the mass density, $\rho = 0.91$ g/cm^3 and c is the concentration (in "phr", or parts per hundred parts of rubber,) of the peroxide. The values of ν from Eq. 17 for the two natural rubber networks are listed in Table 2.

If the free radical crosslinking reaction of NR is accompanied by substantial side reactions, the resulting networks would contain defects, such as chain ends and possibly

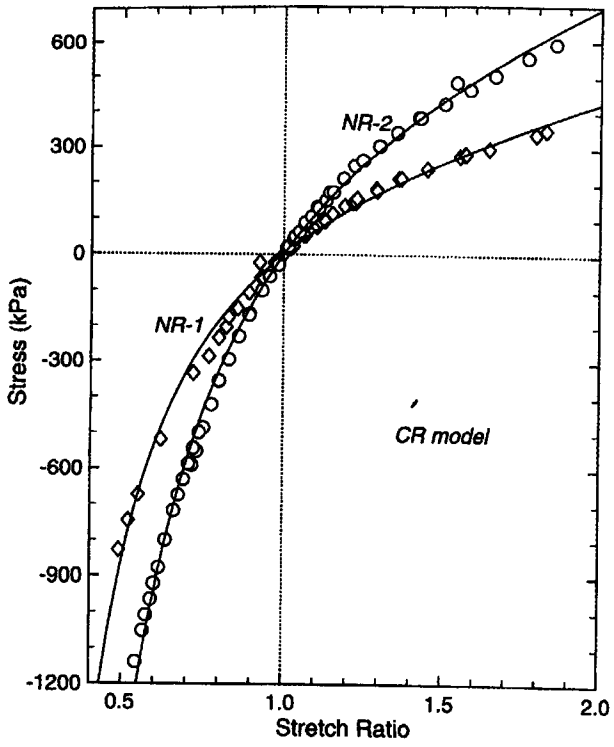

Fig. 2. The natural rubber data of Fig. 1 plotted as the engineering stress versus λ, along with the least-squares fits of the CR model, Eq. 15. The best-fit values of the parameters are listed in Table 1.

inhomogeneity of the crosslink density. A recent study suggested that dicumyl peroxide promotes chain scission during crosslinking of natural rubber [39], which potentially influences the constraint release process modeled by the β parameter in Eq. 15. This would, of course, limit the utility of the comparison in Fig. 2 between model and experiment.

There are no reports of sulfur vulcanization inducing chain scission, and hence analysis of sulfur-crosslinked NR networks is useful. Rivlin and Saunders [40] measured NR vulcanizates over a broad range of strains, using inflation to obtain compression data. These results are reproduced in Fig. 3, along with the least squares best-fit of both Eqs. 11 and 15. For the CC model, agreement with the experimental data is limited to tension, similar to the

Table 1
Results of fitting NR and PBD data

	CC model (Eq. 11)			CR model (Eq. 15)			
	G_c (kPa)	κ	φ	G_c (kPa)	G_e (kPa)	β	G_N (kPa)
NR-1	65	3	4	244	0	~0	360[a]
NR-2	103	3	4	360	62	~0	↓
NR[b]	78	6	4	106	64	0.1	↓
PBD	393 / 429[c]	2 / 1[c]	6	549	30	1	1300[d]

[a] Reference [48].
[b] Sulfur vulcanized natural rubber from reference [40].
[c] Least-squares fit to extension / compression data.
[d] Reference [49].

Table 2
Network chain density (ν, in moles/m^3) of dicumyl peroxide cured natural rubbers

	Wood equation (Eq. 17)	CC model (Eq. 11[a])	Heinrich model (Eq. 15[a])
NR-1	46	52	200
NR-2	110	83	290

[a] Using Eq. 3 (which ignores chain ends) and assuming $\nu = 2\mu$.

results for peroxide-cured NR. The performance of the CR model is comparable for $\lambda > 1$, and superior for the compression data. Values of the various fitting parameters are listed in Table 1.

4.2. Polybutadiene network

Mechanical equilibrium data was obtained for the crosslinked PBD in both tension and compression. This material differs in two principle ways from the NR networks. The junctions of the PBD will have higher functionality, since some chain reaction accompanies free-radical crosslinking of the 1,4-polydiene units [41,42]. This confluence of chains at a junction site should increase the severity of the constraints on the network motion. A second difference between the two materials is the higher plateau modulus of PBD in comparison to NR [28]. This should yield higher values for the fitting parameters, G_N or G_e, of the tube models (Eqs. 14 or 15 respectively), since these quantities

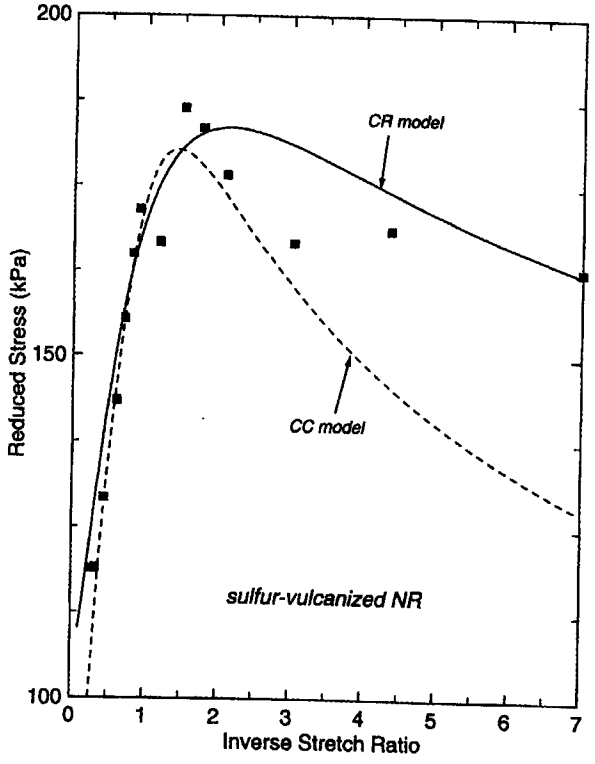

Fig. 3. The data of Rivlin and Saunders [40] for vulcanized natural rubber, along with the best-fit to the CR (Eq. 15) and CC (Eq. 11) models. Agreement with the latter is limited to extension ($\lambda < 1$).

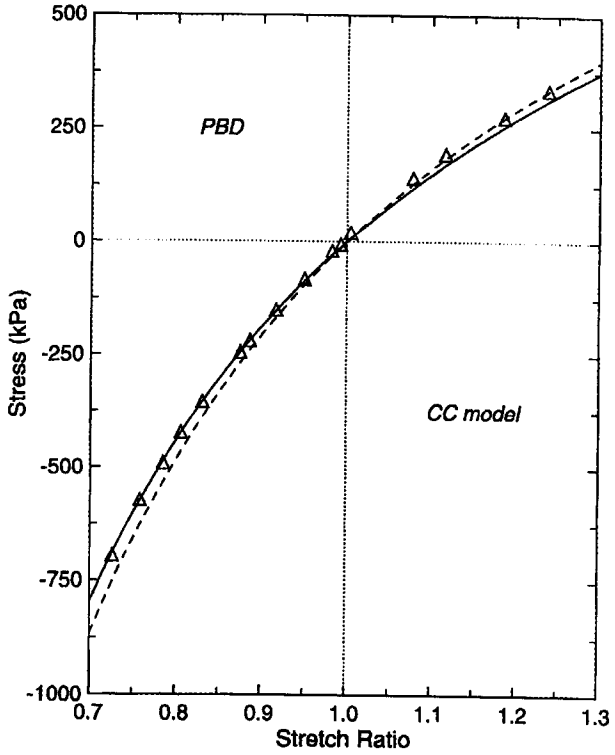

Fig. 4. Best fit of the CC model, Eq. 11, to the data for the PBD network in compression (—; $C_1 = 429$ kPa, $\kappa = 2$, and $\varphi = 6$) and in tension (– – –; $C_1 = 393$ kPa, $\kappa = 1$, and $\varphi = 6$).

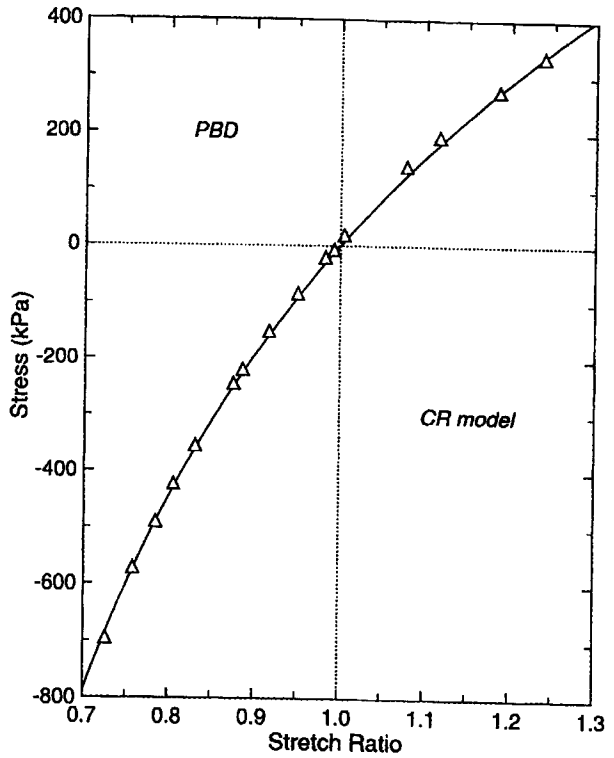

Fig. 5. Best fit of the CR model, Eq. 15, to the PBD network data, yielding $G_c = 549$ kPa, $G_e = 30$, and $\beta = 1$.

reflect the entanglement contribution to the network modulus. Thus, beyond judging the quality with which experimental data can be fit, the values obtained for the fitting parameters per se allow assessment of the models.

In Fig. 4 are displayed the data for the PBD network, along with two fits of the CC model. Similar to the results for NR, tension and compression results can not be described simultaneously. Instead, we show the respective least-squared fits to each individually, with the obtained parameters given in Table 1.

Fig. 5 shows the least-squares fit of the CR model to the same PBD data. Although there is small systematic deviation for extension, the accuracy of the model is relatively good. Certainly Eq. 15 conforms better to the data than does of Eq. 11. However, this may just reflect the availability of an extra adjustable parameter. Thus the models must be judged on physical grounds.

5. Discussion

Referring to Table 2, the CC model (Eq. 11) yields values for the network chain density in good agreement with the ν estimated from the Wood equation, which is based on the peroxide crosslinking reaction (Eq. 17). The CR model, on the other hand, yields overly-large crosslink densities. In comparing the parameters listed in Table 1 for the elastomers, both the crosslink density (viz. G_c) and its functionality (φ) are higher for PBD than for NR-1 or NR-2. We therefore expect motion of the PBD network to be more constrained [43–46]. Contrarily, the parameter G_e, reflecting topological restrictions on the network chains, is lower for PBD than NR-1.

The value of G_c itself is more than an order of magnitude lower than the plateau modulus determined for PBD in the melt [47]. This implies an unrealistically small trapping factor, given that the molecular weight between crosslinks for the PBD is less than its molecular weight between entanglements. Moreover, G_c is lower for PBD than NR (Table 1), although NR has a larger plateau modulus [48]. Such a result is counterintuitive, since the chain propagation accompanying free radical crosslinking of PBD yields $\varphi > 4$, whereas peroxide crosslinking of NR results in tetrafunctional crosslinks [41,42].

For the NR-1, the best fit to the experimental data is obtained using $G_e = 0$. Although such a result is untenable, it parallels earlier work of Heinrich and Kaliske [31,32]. They successfully applied the CR model (Eq. 15) to data on filled rubber subjected to complex shear deformations, although the values obtained for the fitting parameters were unphysical (e.g., negative Ge and β). Clearly, iterative procedures intended to minimize differences with experiment may yield material parameters that are optimal only in a mathematical sense. To remedy this, fitting procedures may be constrained according to knowledge of the material [49,50], although this entails some degradation of the fit quality.

The β values in Table 1 suggest that there is essentially no constraint release accompanying deformation of the PBD. Such behavior can perhaps be reconciled with the PBD's high concentration of crosslinks, which are moreover high in functionality. For all the NR networks herein, the contribution from constraint release is substantial ($\beta \sim 0$). In the context of the model, this implies global rearrangement of the network, engendering strong departures from affine deformation.

6. Conclusion

Accurate constitutive equations can be quite useful for finite-element modeling, which requires stress-strain relations over a broad range of deformations. However, the success of molecular models is mitigated if the obtained parameters do not offer meaningful physical insights. Models whose usefulness is limited to their accuracy should be compared to semi-empirical approaches. There are a number of functions [51–54] which perform quite well in this regard. There are also the phenomenological "chain models" [55–59], which rely on non-Gaussian statistics (e.g., the inverse Langevin function [6,7]) to obtain stress-strain laws valid for large deformations. While practical use can be made of these, the search nevertheless continues for rigorous molecular models which have sufficient utility. The models described herein all represent different realizations of the same idea — that topological constraints influence the microscopic deformation. This concept is certain to be an central feature of further theoretical advancements.

Acknowledgements

The work at NRL was supported by the Office of Naval Research. GH thanks Continental AG for permission to publish.

References

[1] Mott PH, Roland CM. Rubber Chem Technol 1995;68:739.
[2] Mott PH, Roland CM. Macromolecules 1996;29:6941.
[3] Roland CM, Mott PH. Macromolecules 1998;31:4033.
[4] Gottlieb M, Macosko CW. Macromolecules 1982;15:535.
[5] Gottlieb M, Gaylord R. Polymers 1983;24:1644.
[6] Treloar LRG. The physics of rubber elasticity. Oxford, UK: Clarendon Press, 1975.
[7] Treloar LRG. Rep Prog Phys 1973;36:755.
[8] Erman B, Mark JE. Structures and properties of rubberlike networks. New York: Oxford University Press, 1997.
[9] Rivlin RS. Rubber Chem Technol 1992;65:G51.
[10] Flory PJ. Polymer 1979;20:1317.
[11] Allen G, Kirkham MJ, Padget J, Price C. Trans Faraday Soc 1971;67:1278.
[12] Erman B, Mark JE. Macromolecules 1987;20:2892.
[13] Roland CM. Rubber Chem Technol 1989;62:863.
[14] Wagner MHJ. Rheology 1994;38:655.
[15] Larson RG. Constitutive equations for polymer melts and solutions. Boston: Butterworths, 1988.
[16] Wagner MH, Schaeffer JJ. Rheology 1993;37:643.
[17] James HM, Guth EJ. J Chem Phys 1953;21:1039.
[18] Flory PJ. Macromolecules 1982;15:99.
[19] Flory PJ. Proc Royal Soc London A 1976;351:351.
[20] Flory PJ. J Chem Phys 1977;66:5720.
[21] Flory PJ, Erman B. Macromolecules 1982;15:800.
[22] Erman B. and Monnerie L. Macromolecules 1989;22:3342; 1992;25:4456.
[23] Kloczkowski A, Mark JE, Erman B. Macromolecules 1995;28:5089.
[24] Kloczkowski A, Mark JE, Erman B. Computational Polym Sci 1995;5:37.
[25] Doi, M, Edwards SF. The Theory of Polymer Dynamics. Oxford: Clarendon Press, 1986.
[26] Dossin LM, Graessley WW. Macromolecules 1979;12:123.
[27] Langley NR. Macromolecules 1968;1:348.
[28] Ferry JD. Viscoelastic properties of polymers. NY: Wiley, 1980.
[29] Rubinstein M, Panyukov S. Macromolecules 1997;30:8036.
[30] Heinrich G, Straube E, Helmis G. Adv Polym Sci 1988;85:33.
[31] Heinrich G, Kaliske M. Comp Theor Polym Sci 1997;7:227.
[32] Kaliske M. and Heinrich G. Rubber Chem Technol, to appear 1999.
[33] Schroeder MJ, Roland CM. Macromolecules 1999; in press.
[34] Pearson DS. Rubber Chem Technol 1987;60:439.
[35] Graessley WW. Adv Polym Sci 1982;47:68.
[36] Gent AN. In: Mark JE, Erman B, Eirich FR, editors. Science and Technology of Rubber, San Diego: Academic Press, 1994 Ch. 1.
[37] McKenna GB, Zapas LJ. Polymer 1983;24:1502.
[38] Wood LA. Rubber Chem Technol 1977;50:233.
[39] Pyckhout-Hintzen, W., unpublished results.
[40] Rivlin RS, Saunders DW. Phil Trans Royal Soc London A 1951;243:251.
[41] Coran AY. In: Ehrich FR, editor. Science and technology of rubber. New York: Academic Press, 1978, Ch. 7.
[42] Bohm GGA, Tveekrem JO. Rubber Chem Technol 1982;55:575.
[43] Flory PJ, Erman BJJ. Polym Sci Polym Phys Ed 1984;22:1953.
[44] Sanjuan J, Llorente MAJ. Poly Sci Poly Phys Ed 1988;26:235.
[45] Ngai KL, Roland CM, Yee AF. Rubber Chem Technol 1993;66:817.
[46] Ngai KL, Roland CM. Macromolecules 1994;27:2454.
[47] Roland CM, Kallitsis JK, Gravalos KG. Macromolecules 1993;26:6474.
[48] Santangelo PG, Roland CM. Macromolecules 1998;31:3715.
[49] Yeoh OH. Rubber Chem Technol 1997;70:175.
[50] Marzocca AJ, Cerveny S, Raimondo RBJ. Appl Polym Sci 1997;66:1085.
[51] Ogden RW. Proc Roy Soc A 1972;326:565.
[52] Valanis KC, Landel RFJ. Appl Phys 1967;38:2997.
[53] Martin GM, Roth FL, Stiehler RD. Trans Inst Rub Ind 1956;32:189.
[54] Landel RF. Rubber Chem Technol 1998;71:234.
[55] Arruda EM, Boyce MCJ. Mech Phys Solids 1993;41:389.
[56] Arruda EM, Przybylo PA. Polym Eng Sci 1995;35:395.
[57] Gent AN. Rubber Chem Technol 1996;69:59.
[58] Boyce MC. Rubber Chem Technol 1996;69:781.
[59] Yeoh OH, Fleming PDJ. Polym Sci Polym Phys 1997;35:1919.